

RENDICONTI LINCEI MATEMATICA E APPLICAZIONI

CRESCENTINO BOSCO, ALBERTO CARPINTERI

Fracture mechanics as applied to plain and reinforced concrete with particular reference to scaling of experimental data

Atti della Accademia Nazionale dei Lincei. Classe di Scienze Fisiche, Matematiche e Naturali. Rendiconti Lincei. Matematica e Applicazioni, Serie 9, Vol. 1 (1990), n.4, p. 351–366.

Accademia Nazionale dei Lincei

[<http://www.bdim.eu/item?id=RLIN_1990_9_1_4_351_0>](http://www.bdim.eu/item?id=RLIN_1990_9_1_4_351_0)

L'utilizzo e la stampa di questo documento digitale è consentito liberamente per motivi di ricerca e studio. Non è consentito l'utilizzo dello stesso per motivi commerciali. Tutte le copie di questo documento devono riportare questo avvertimento.

Atti della Accademia Nazionale dei Lincei. Classe di Scienze Fisiche, Matematiche e Naturali. Rendiconti Lincei. Matematica e Applicazioni, Accademia Nazionale dei Lincei, 1990.

Meccanica dei solidi. — *Fracture mechanics as applied to plain and reinforced concrete with particular reference to scaling of experimental data.* Nota di CRESCENTINO BOSCO e ALBERTO CARPINTERI, presentata (*) dal Socio E. GIANGRECO.

ABSTRACT. — Whereas in elasticity and plasticity geometrically similar structures behave in the same way, when strain-softening and strain-localization are taken into account the structural behaviour ranges from ductile to brittle merely by increasing size and keeping material properties and geometrical shape unchanged. The size-scale of plain and reinforced concrete elements has often revealed a fundamental influence on the global structural behaviour. This has been theoretically predicted and experimentally confirmed by the results obtained so far. As a consequence this is likely to influence several aspects concerning the design of large structures. The paper emphasizes how the size effects are also present in R.C. elements with a low content of steel and outlines the implications on the minimum steel percentage for these structures.

KEY WORDS: Fracture mechanics; Concrete structures; Size effects; Brittleness number; Minimum reinforcement.

RIASSUNTO. — *Applicazioni della meccanica della frattura al calcestruzzo semplice e rinforzato con particolare riferimento agli effetti di scala.* Mentre nel campo elastico e in quello plastico le strutture geometricamente simili hanno lo stesso comportamento, quando si considerano il ramo discendente della curva sforzi-deformazioni e la localizzazione delle deformazioni, il comportamento strutturale passa da duttile a fragile semplicemente modificando le dimensioni e lasciando inalterata la forma geometrica. Si riscontra quindi come l'effetto scala abbia una importanza fondamentale sul comportamento strutturale globale delle strutture di calcestruzzo semplice ed armato. Tale fenomeno, previsto teoricamente è confermato dai risultati sperimentali finora ottenuti dagli autori e può influenzare diversi aspetti riguardanti il progetto delle strutture. Il presente lavoro mette in evidenza come l'effetto scala sia presente anche nelle travi di calcestruzzo armato aventi basso contenuto di acciaio e ne delinea le implicazioni sulla percentuale minima di armatura per tali strutture.

1. INTRODUCTION

Several materials used in civil engineering, in particular concrete, present softening in their ultimate behaviour under loading. This means that, after the elastic, hardening and/or plastic stages, the load sustained by the material element begins to decrease even though the deformation is ulteriorly increased. Experimental tests revealed that materials with aggregates follow elastic-softening constitutive laws: as a consequence, beyond a certain strain level, the mechanical behaviour of a not homogeneous structural component, is accompanied by strain-localization within a damage zone. The descending branch of the load-deformation curve is experimentally detected if the loading process is strain-controlled.

The size-scale of the structural component has often revealed a fundamental influence on the global behaviour. In fact, whereas in elasticity and plasticity geometrically

(*) Nella seduta del 21 aprile 1990.

similar structures behave in the same way, when strain softening and strain-localization are taken into account the structural behaviour ranges from ductile to brittle merely by increasing size and keeping material properties and geometrical shape unchanged. This result may be explained considering that in classical elasticity and plasticity only energy dissipation per unit of volume is allowed, while, if energy dissipation per unit of area is also considered (*i.e.* strain or curvature localization), the global brittleness becomes scale-dependent.

The discipline of Fracture Mechanics considers cracks as inherent parts of the system, that can affect the strength of materials and structures. The presence of cracks involves discontinuity, reducing the effectiveness of a material to transmit stress locally and then a transition from a continuous to a discontinuous system appears. The introduction of parameters which explicitly refer to developing free surfaces, such as G_F , fracture energy, is then needed, particularly when investigation on large structures is requested (deep beams, as well as dams and nuclear vessels).

Although in the 1970's many features of aggregative materials have not encouraged the application of Fracture Mechanics to analyse plain and reinforced concrete structures, a few authors [1-9] have recently analysed their behaviour using the concepts of this discipline, both employing linear or non linear analysis. The results revealed that above certain structural sizes and for particular values of steel percentage, even reinforced concrete may result to be sufficiently brittle, or, in other words, it does present a transition between ductile and brittle behaviour. Fracture sensitivity, in fact, is not an intrinsic material property, but it depends on the size of the structure where the crack is localized.

The present paper summarizes the experimental results obtained so far by the writers, that show how the theoretical trends predicted by LEFM are experimentally confirmed, not only for plain concrete but even for reinforced concrete elements. As a matter of fact, it is possible to define a dimensionless number [7, 9], which can represent, for each concrete strength, different behaviours, *i.e.* from ductile to brittle collapse. Such number is a function of cross-section size for plain concrete, whereas it also depends on steel percentage for reinforced concrete.

In particular the test results recently obtained in [10-11] for concrete structures in flexure, could be profitably applied to estimate the minimum reinforcement percentage, this parameter being scale-dependent.

2. SIZE EFFECT

Size-effects may easily be observed in tensile tests on concrete specimens, where the damaged zone is more and more localized as the loading capacity decreases. In fact, while the material within the fracture zone softens, (fig. 1a), stress and strain in the undamaged portion of the material still behave in a proportional manner. As a consequence, strains accumulate in the fracture zone, while the remaining part of the structure unloads itself.

A well known representative model [12], assumes that the original length of the

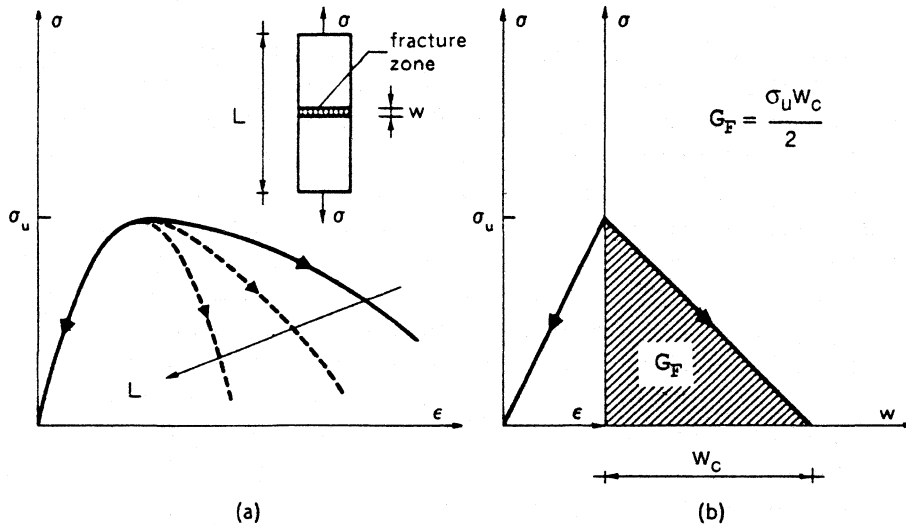


Fig. 1. - Stress-displacement law for softening materials.

fracture zone in the tensile direction is equal to zero, whereas it is different from zero while it is actually developing. The stress at the softening stage, therefore, will be a function of such a length w , (fig. 1b). This simple hypothesis explains the size effect for the descending branch of the σ - ϵ curve, which appears varying with specimen length (fig. 1a).

Another remarkable consequence of this hypothesis, widely confirmed in practice, is that it is possible to have similarity in the physical fracture behaviour when the value w_c of a total stress relaxation is proportional to the structural size L , *i.e.* when the fracture energy $G_F \approx \sigma_u w_c / 2$ is proportional to L . In such a case, the global collapse dilatation $\epsilon_c \approx w_c / L$ appears to be constant as the size L is varied.

The area under the σ - ϵ curve represents energy dissipated per unit of volume, thus having the physical dimension of stress $[FL^{-2}]$, while the area under the σ - w curve represents energy dissipated per unit of area, thus having the dimension of surface energy $[FL^{-1}]$. The latter area represents the fracture energy G_F , *i.e.* the energy necessary to create a unit free surface. The relation $K_{IC} = (G_F E)^{1/2}$ gives another fracture toughness parameter, the critical stress intensity factor, being E the Young's modulus of the material.

In a cracked member with fixed geometrical ratios, two kinds of failure mechanisms can occur:

- (1) ultimate strength collapse, when the highest normal stress σ in the body reaches the maximum value and the crack is only considered as a weakening for the cross-section. If the material is elastic-perfectly plastic, the yield strength $\sigma = \sigma_p$ will be used as a reference in the limit analysis, while the tensile strength $\sigma = \sigma_u$ will be considered for elastic-brittle constitutive laws;
- (2) propagation of an initial crack, induced by the critical value of the stress intensity factor $K_I = K_{IC}$.

The two mechanisms of collapse are respectively represented by the critical values of the parameters σ (σ_u in brittle strength collapse or σ_p in plastic collapse) and K_{IC} (catastrophic collapse), which differ in physical dimensions.

The characteristic number

$$(1) \quad s = K_{IC}(\sigma_u b^{1/2})^{-1},$$

called brittleness number [2, 13, 14], correlates the ultimate strength collapse when $s > s_0$ and the brittle collapse in the opposite situation. The threshold s_0 depends on the geometry of the test specimen. For the three point bending test the critical brittleness number s_0 has been evaluated in [13] and fig. 2 clearly shows that the failure of a structural element can be evaluated by means of limit analysis only if $s > 0.5$ (zone above the bold line), while in the lower part of the diagram crack propagation precedes ultimate strength collapse. An elastic-brittle material has been considered in fig. 2. On the other hand equivalent results would be obtained for elastic-perfectly plastic constitutive laws.

A brittleness number

$$(2) \quad N_p = f_y b^{1/2} A s (K_{IC} A)^{-1},$$

has also been defined for cracked reinforced concrete elements [7, 9]. A rigid-plastic constitutive law is assumed for steel, while for concrete a linear-elastic law, coupled with a fracturing condition according to LEFM is utilized. The mechanical

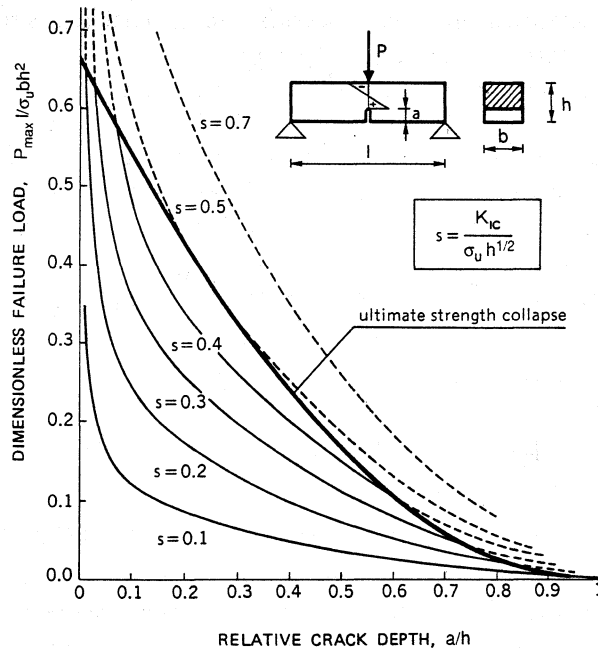


Fig. 2. – Interaction between strength collapse and separation collapse for three point bending tests (plain concrete).

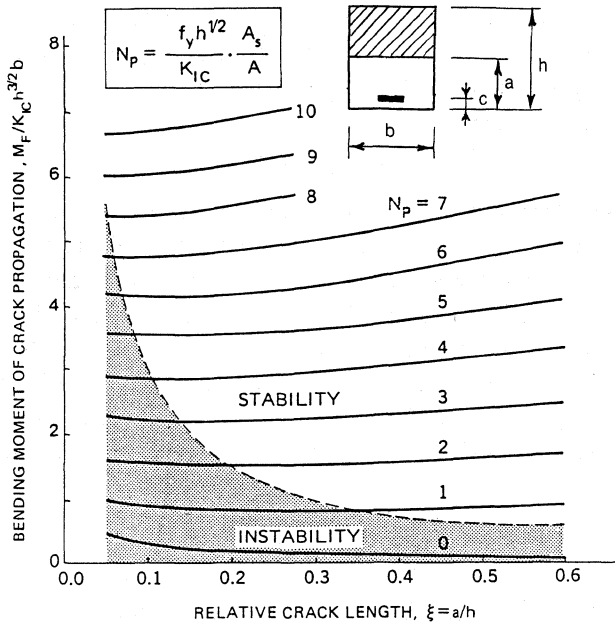


Fig. 3. – Bending moment of concrete fracture varying the brittleness number N_p (reinforced concrete, with $c = b/20$).

parameters characterizing the two materials are f_y (yielding strength of steel) and K_{IC} (critical stress intensity factor of concrete).

The bending moment of crack propagation is represented in fig. 3 by varying the non-dimensional number N_p . It is possible to notice how the fracturing process can be stable or unstable even for reinforced concrete elements, the dashed line dividing the two conditions. In particular, the fracturing process is stable only when the beam is sufficiently reinforced and/or the cross-section is sufficiently small, and when the crack is sufficiently deep.

The behaviour of a cracked reinforced concrete cross-section, as it is described by the model, can then be summarized as follows.

(A) The response is rigid until the moment of steel yielding is reached. The local rotation is zero.

(B) Linear hardening behaviour follows when the applied moment is greater than the moment of steel yielding.

(C) The latter stops when the moment of crack propagation is reached.

If the fracture process is unstable, *i.e.* for low N_p values, a complete and instantaneous disconnection of concrete occurs. Then the diagram moment *vs.* rotation $M-\phi$, presents a discontinuity and jumps to the moment given by the plastic steel reaction times the internal lever arm. On the other hand, an increasing moment-rotation diagram appears if the fracture process is stable, *i.e.* for high N_p values. The transitional

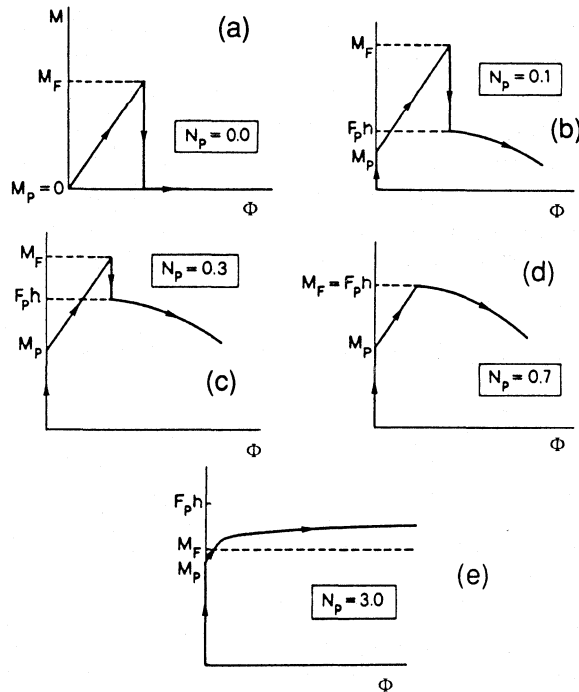


Fig. 4. – Ductile-brittle transition in the mechanical behaviour of reinforced concrete beams, by varying the brittleness number N_p .

limit is observed when the moment of crack propagation is approximately equal to $F_p b$, F_p being the force transmitted by the yielded steel and b the distance of steel from the compressive edge of the beam. The sequence of the diagrams $M-\phi$ by increasing N_p is reported in fig. 4.

The existence of a transitional value N_{PC} then clearly appears, as well as the possibility, based on this parameter, to evaluate stability or instability in the behaviour of reinforced concrete elements in flexure.

3. SPECIMEN PREPARATION AND TESTING PROCEDURE ON R.C. BEAMS

The experimental tests were carried out at the Department of Structural Engineering of the Politecnico of Torino.

A first series of 30 high strength concrete beams was planned with the main purpose to verify the existence of size effects in those structural elements. Subsequently 38 beams with three different concrete grades were planned to determine, for each concrete grade, the transitional limit between ductile and brittle failure by varying the scale. In the latter case, therefore, the purpose was to determine the transitional N_{PC} value for a given concrete strength.

The cross-section of the 68 beams presents thickness $b = 150$ mm and depth $h = 100, 200, 400$ mm, for the specimens A, B, C respectively, and thickness $b = 200$ mm and depth $h = 800$ mm, for the specimens D (see table I). The content of steel depends on the beam size and the selected brittleness number, see eq. (1) and table I. The longitudinal steel reinforcement, arranged at a distance $b/10$ from the beam edge, is constant over the entire length of the beam. There is no transverse shear reinforcement and the maximum aggregate diameter is 13 mm.

The three point bending tests on initially uncracked beams were realised by a servocontrolled machine. The beams were supported by a cylindrical roller and a spheri-

TABLE I. - Description of the R.C. specimens: brittleness number, actual content of steel (%), mechanical and toughness characteristics.

Brittleness number	Beam type, cross-section sizes and span (mm)				Mechanical and toughness characteristics			
	A	B	C	D	f_{cm} (N/mm ²)	E_C (N/mm ²)	G_F (N/mm)	K_{IC} (N/mm ^{3/2})
N_p	150 × 100	150 × 200	150 × 400	200 × 800				
	600	1200	2400	4800				
Percentage of steel								
(a) Concrete grade 0 (1988)								
0.00	0	0	0	—				
0.10	0.085	0.064	0.043	—				
0.26	0.256	0.190	0.128	—	75.70	34300	0.090	55.56
0.53	0.653	0.490	0.327	—				
0.87	1.003	0.775	0.517	—				
(b) Concrete grade I (1989)								
0.11-0.15	0.131	0.094	0.083	0.049				
0.23-0.30	0.261	0.188	0.167	0.098	16.63	21000	0.143	54.80
0.35-0.45	0.392	0.283	0.250	0.147				
(c) Concrete grade II (1989)								
0.11-0.15	0.131	0.094	0.083	0.049				
0.23-0.30	0.261	0.188	0.167	0.098	29.38	23150	0.134	55.70
0.35-0.45	0.392	0.283	0.250	0.147				
(d) Concrete grade III (1989)								
0.11-0.15	0.131	0.094	0.083	0.049				
0.23-0.30	0.261	0.188	0.167	0.098	39.45	25590	0.139	64.15
0.35-0.45	0.392	0.283	0.250	0.147				

cal connection respectively at the two extremities (span = 6 times the depth b). The load was applied in the midspan through a hydraulic actuator and the loading process was controlled by a strain gage type DD1, placed on the lower beam edge, symmetrically with respect to the force and parallel to the beam axis; its length was equal to the beam depth, *i.e.* 100, 200, 400 or 800 mm, respectively for the beam sizes *A*, *B*, *C* and *D*. After cracking the loading process was controlled by the crack mouth opening displacement. The strain rate was imposed at a constant and very low value, so that the crack formation in the middle of the beam was achieved after about 7 minutes and the steel yielding after about 45 minutes, on the average. Even the compressive and tensile strains on the upper and lower edges of the beam were recorded. The measured central deflection was referred to a bar, connected with the concrete beam at the middle of the depth and in correspondence of the two supports. Deflection and strain gage deformations were plotted automatically as functions of the applied load.

The fracture energy G_F was determined on three specimens for each concrete grade according to the method specified in the RILEM draft recommendation «Determination of the fracture energy of mortar and concrete by means of three-point bend tests on notched beams». The value of the normal elastic modulus was determined according to the method specified in ISO 6784. Concrete cubic strength was considered to be equal to the mean of the results obtained on six $16 \times 16 \times 16$ cm test cubes for each concrete grade. The cylindrical strength f_{cm} of concrete is reported in table I.

The mechanical properties of the high bond steel reinforcement are listed in table II, where f_t is the ultimate tensile strength, f_y represents the yielding strength and A_5 the elongation at failure on a 5 diameter base. A general view of the four beam size-scales is given in fig. 5.

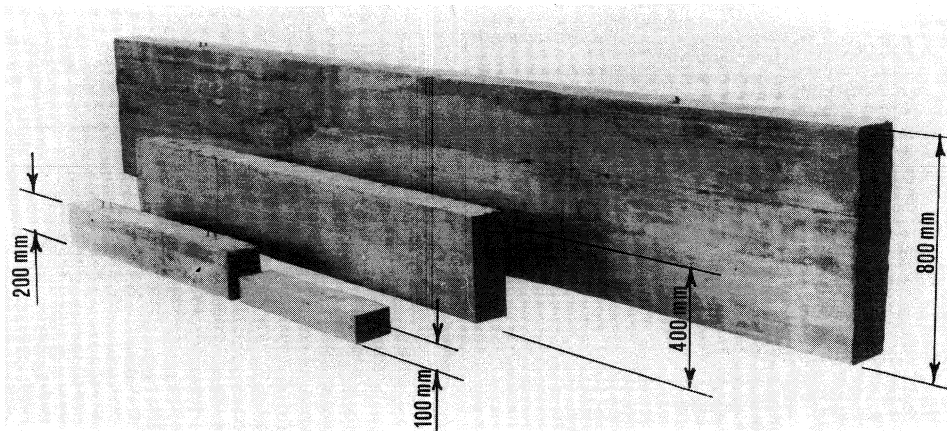


Fig. 5. - View of the four beam size-scales.

TABLE II. - Mechanical characteristics of high bond steel reinforcement.

	Diameter of the 1st series (mm)				Diameter of the other series (mm)			
	4	5	8	10	5	6	8	10
f_t (N/mm ²)	680	622	675	580	673	668	704	562
f_y (N/mm ²)	637(*)	569(*)	441	456	633(*)	489	480	456
A_s (%)	20	22	30	32	24	32	33	30

(*) Obtained from stress-strain diagram at 0.2% of permanent deformation.

4. EXPERIMENTAL RESULTS AND DISCUSSION

For the first series of beams, the dimensionless bending moment *vs.* rotation diagrams are plotted in the figs. 6 *a* to *e*, for each brittleness class and by varying the beam size. The local rotation is non-dimensionalized with respect to the value ϕ_0 recorded at the first cracking, and is related to the central beam element of length equal to the beam depth *b*. The bending moment, on the other hand, is non-dimensionalized with respect to the critical value of stress intensity factor of concrete, K_{IC} , and the beam depth *b*.

The diagrams in fig. 6 are significant only for $\phi/\phi_0 > 1$, the strain softening and curvature localization occurring only after the first cracking. The dimensionless peak moment does not appear to be the same, when the brittleness class is the same and the beam depth is varied. This is due to the absence of an initial crack or notch. On the other hand, the post-peak branches are very close to each other and present the same shape for each selected brittleness class. The size-scale similarity seems then to govern the post-peak behaviour, specially for low brittleness numbers N_p .

The moment-rotation diagrams for the beams of the second series are reported in fig. 7. The same indications of size-scale similarity are obtained even from these results [11]. It is worth noting that, due to the different purpose of the experimental investigations subsequent to the first series, the N_p values present an high variability, changing the beam depth (in the last tests in fact, the goal was to approximate the transitional N_{pC} value, while in the first ones it was to verify the existence of the size-scale effects). This fact explains the larger dispersion of the curves.

In any case the results demonstrate that the size-scale effect, theoretically predicted by the model, is experimentally confirmed not only for high strength concrete, but even for concrete strengths normally used in civil structures.

The load-deflection diagrams, for the first series of beams, are plotted in the figs. 8 *a*, *b* and *c*, for each beam size and by varying the brittleness number from zero to 0.87.

As it is possible to verify, the peak of first cracking load is decidedly lower than the steel yielding load only in the cases 3 and 4, *i.e.* for high brittleness numbers N_p . In the cases 0 and 1, the opposite result is clearly obtained. On the other hand, case 2 demonstrates to represent a transitional condition between brittle and plastic collapse, the two critical loads being very close. Therefore, the same brittleness transition theoretically predicted in fig. 4, is reproduced by the experimental diagrams in figs. 8.

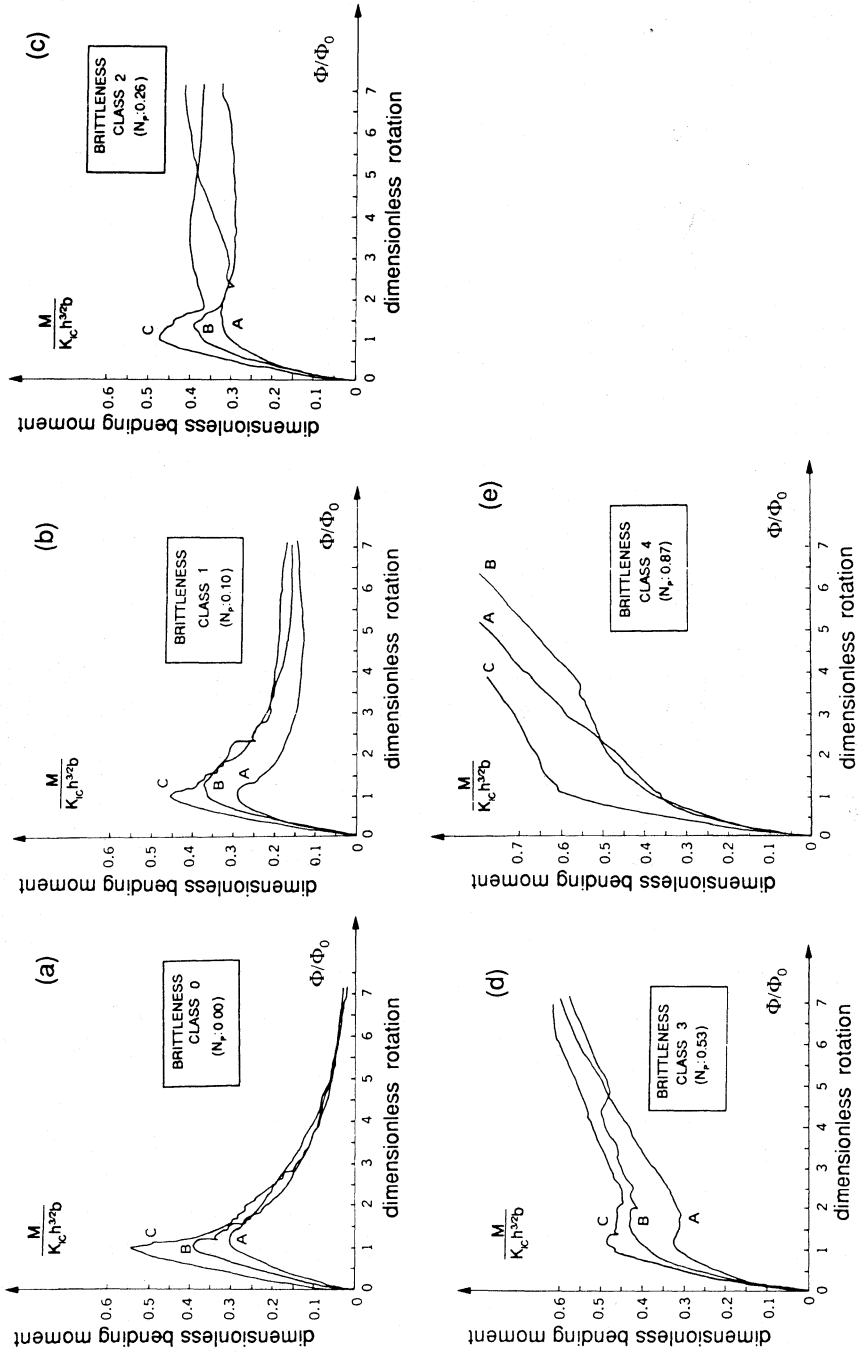


Fig. 6. - Dimensionless bending moment vs. rotation diagrams for the first series of beams. Brittleness number: $N_p \approx 0.00$ (a); $N_p \approx 0.10$ (b); $N_p \approx 0.26$ (c); $N_p \approx 0.53$ (d); $N_p \approx 0.87$ (e). Beam depth: (A) $b = 100$ mm; (B) $b = 200$ mm; (C) $b = 400$ mm.

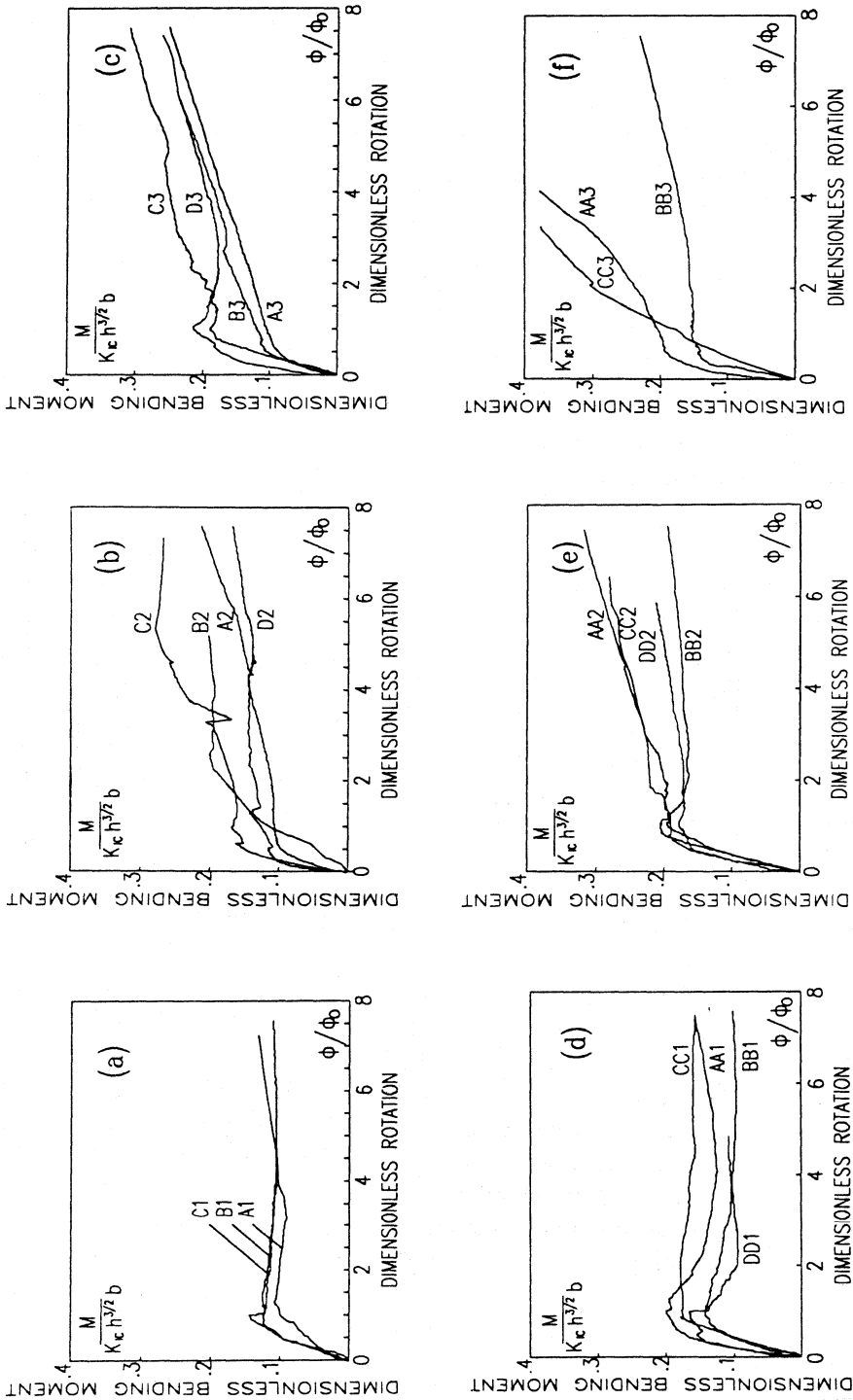


Fig. 7. - Dimensionless bending moment vs. rotation diagrams for the beams of the second series. Beam type I: brittleness class $N_p \approx 0.11-0.15$ (a); $N_p \approx 0.23-0.30$ (b); $N_p \approx 0.35-0.45$ (c). Beam type II: brittleness class $N_p \approx 0.11-0.15$ (d); $N_p \approx 0.23-0.30$ (e); $N_p \approx 0.35-0.45$ (f). Beam depth: (A), (AA) $b = 100$ mm; (B), (BB) $b = 200$ mm; (C), (CC) $b = 400$ mm; (D), (DD) $b = 800$ mm.

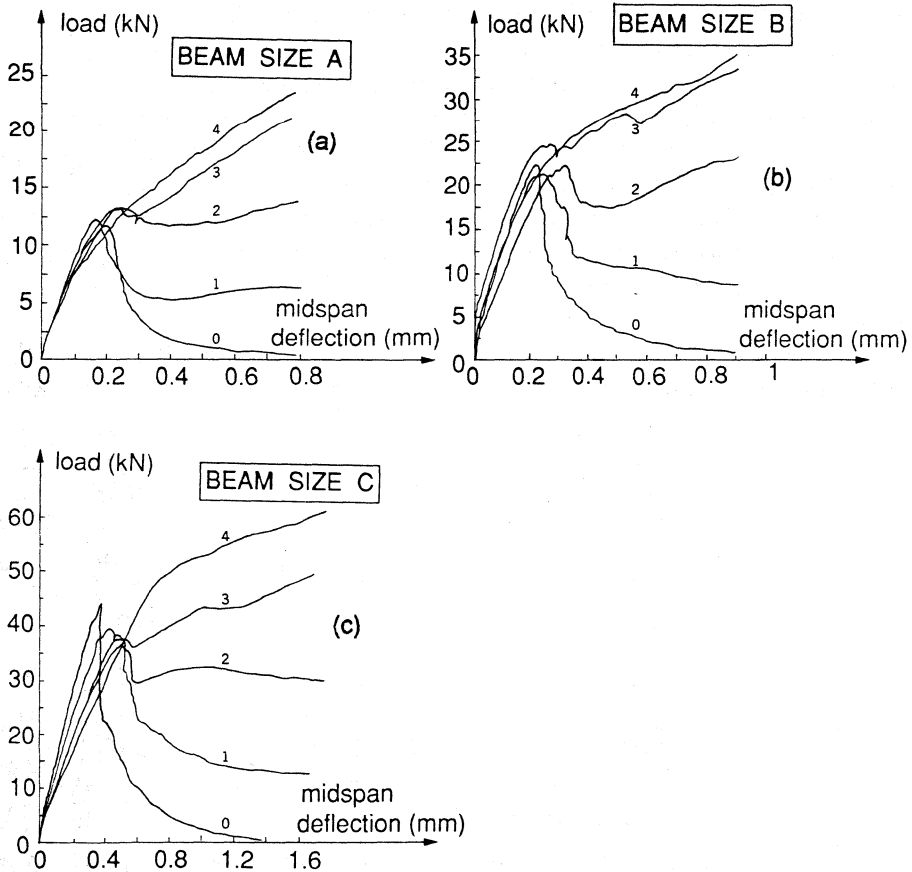


Fig. 8. - Load vs. deflection diagram for the first series of beams. (a) beam depth $b = 100$ mm; (b) beam depth $b = 200$ mm; (c) beam depth $b = 400$ mm.

Moreover, taking into account the previous considerations and then observing again figs. 6 and 7, it is possible to infer that the brittleness number for which the transition occurs, is constant for a given concrete grade.

It is still interesting to observe that in some cases the softening branch in the curves $P-\delta$ revealed a positive slope (snap-back behaviour). It was possible to follow such a branch, since the loading process was controlled by a monotonically increasing function of time, *i.e.* the crack mouth opening displacement. If the controlling parameter had been the central deflection, a sudden drop in the loading capacity and an unstable and fast crack propagation would have occurred.

5. MINIMUM REINFORCEMENT

From the experimental investigation described above, a typical load-deflection diagram was obtained, as shown in fig. 9. This is characterized by two peaks, *A* and *Y*,

related to the moments of first cracking M_A and steel yielding M_Y . The curve (b) represents the transition between the unstable (a) and stable (c) behaviour.

In statically determined structures, the minimum reinforcement percentage must be calculated with reference to the onset of cracking. If the structure is redundant, on the contrary, a loading redistribution takes place in the section where the crack first appears, the moment decreasing to an extent that varies depending on the overall configuration of the structure. The same applies also when cracking is caused by imposed deformations. In this case the decrease of the bending moment makes it possible to calculate the minimum steel content on the basis of a reduced value of the cracking moment.

Therefore, being necessary to guarantee that the reinforcement will not reach the yield point up to the formation of the first crack ($M_Y \geq M_A$), the transitional N_{PC} value

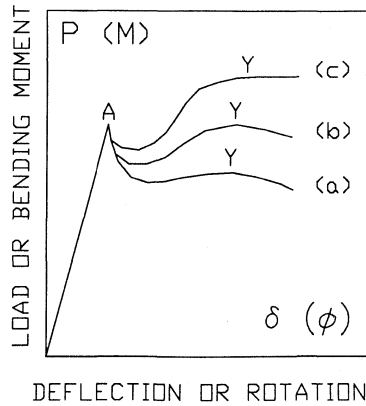


Fig. 9. - Load vs. deflection diagrams for low reinforced concrete beams.

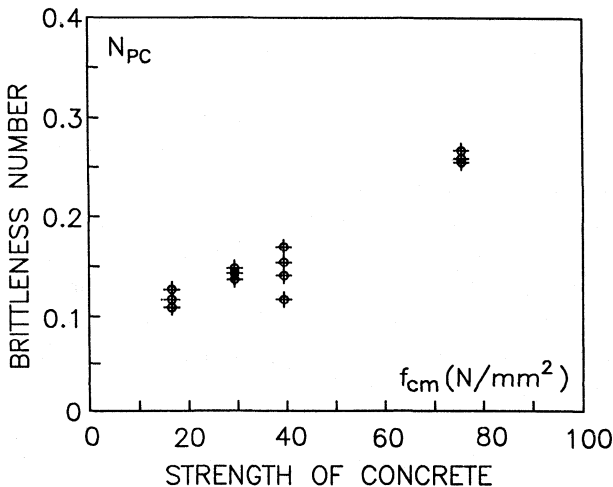


Fig. 10. - Transitional brittleness number N_{PC} against the cylindrical compression strength of concrete.

is represented by the limit condition $M_Y = M_A$. On the other hand, the experimental results obtained so far show that the transitional value of the brittleness number, N_{PC} , is markedly constant for each concrete grade, by varying the beam depth b . As a consequence, the determination of the minimum steel percentage, is allowed on the basis of the brittleness number N_p [15].

To represent the transitional brittleness number N_{PC} we can refer to the experimental diagram shown in fig. 10, which indicates how N_{PC} , as an average, increases monotonically against the compressive strength of concrete.

Figure 11 provides the minimum reinforcement percentage, A_s/A , obtained from relation (2), as a function of beam depth b , for the most common concrete strength in structural applications. In the same diagram, the minimum steel percentages requested by the Eurocode 2 [16] and ACI [17], are reported.

While the values supplied by both the standards mentioned above and by several international codes [18], are independent of the beam depth b , the relationship which is established by the brittleness number N_{PC} , calls for decreasing minimum steel percentages with increasing beam depths.

6. CONCLUSIONS

The analysis of the post-peak and ductile behaviour of low reinforced concrete beams, through the concepts of fracture mechanics, provides interesting results, such as the possibility of extrapolating predictions from small to large scales, using an appropriate non dimensional number, where, in addition to the traditional geometrical and mechanical parameters, even the concrete fracture toughness K_{IC} , or the concrete fracture energy G_F , appears.

In addition to the well known result that the brittleness of plain concrete is a function of size [2], the experimental results presented above show that, even in the case

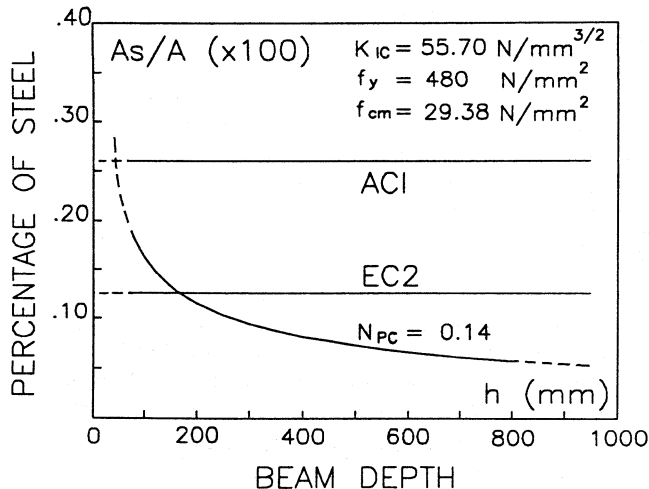


Fig. 11. - Minimum steel percentage against the beam depth b .

of reinforced concrete members in flexure, the brittleness increases by increasing the size and/or decreasing the steel content.

On the other hand, for each concrete grade, a physically similar behaviour is revealed in the cases where the brittleness number N_p is the same. Only when the steel percentage is inversely proportional to the square root of the beam depth, the mechanical behaviour is reproduced. Thus a criterion to evaluate the minimum percentage of reinforcement can be introduced. Such a percentage, assumed to be provided by the condition of simultaneous first cracking and steel yielding, results to be scale-dependent, whereas the current standard codes suggest, for direct loading, values independent of the beam depth.

ACKNOWLEDGEMENTS

The Department of Public Education (M.P.I.) is acknowledged for the financial support provided to the present research.

The authors are grateful to Mr. Orlando Grindatto for his help in carrying out the testing program.

REFERENCES

- [1] A. CARPINTERI, *Scale effects in fracture of plain and reinforced concrete structures*. In: *Fracture Mechanics of Concrete: Structural Application and Numerical Calculation*. Martinus Nijhoff Publishers, Dordrecht-Boston-Lancaster 1985, 95-140.
- [2] A. CARPINTERI, *Notch sensitivity in fracture testing of aggregative materials*. Eng. Fracture Mech., 16, 1982, 467-481.
- [3] Z. P. BAZANT - L. CEDOLIN, *Fracture mechanics of reinforced concrete*. J. of Eng. Mech. Division (ASCE), 106, 1980, 1287-1306
- [4] V. E. SAOUMA - A. R. INGRAFFEA, *Fracture mechanics analysis of discrete cracking*. IABSE Colloquium on *Advanced Mechanics of Reinforced Concrete*, Delft 1981, 413-436 (Final Report).
- [5] P. E. PETERSSON - P. J. GUSTAVSSON, *A model for calculation of crack growth in concrete-like materials*. In: D. R. J. OWEN - A. R. LUXMOORE (eds.), *Numerical methods in Fracture Mechanics*. Pineridge Press, 1980, 707-719.
- [6] A. HILLERBORG, *Fracture mechanics concepts applied to moment capacity and rotational capacity of reinforced concrete beams*. Eng. Fracture Mech., vol. 35, No. 1/2/3, 1990, 233-240.
- [7] A. CARPINTERI, *A fracture mechanics model for reinforced concrete collapse*. IABSE Colloquium on *Advanced Mechanics of Reinforced Concrete*, Delft 1981, 17-30.
- [8] L. ELFGREN (ed.), RILEM REPORT, *Fracture Mechanics of Concrete Structures. From Theory to Applications*. Chapman and Hall, 1989, 191-220.
- [9] A. CARPINTERI, *Stability of fracturing process in RC beams*. J. of Structural Eng. (ASCE), 110, 1984, 544-558.
- [10] C. BOSCO - A. CARPINTERI - P. G. DEBERNARDI, *Fracture of reinforced concrete: scale effects and snap-back instability*. Presented at the Int. Conf. on *Fracture and Damage of Concrete and Rock* (4-6/7/1988), Vienna (Austria); Eng. Fracture Mech., vol. 35, 4/5, 1990, 665-677.
- [11] C. BOSCO - A. CARPINTERI - P. G. DEBERNARDI, *Size effect on the minimum steel percentage for reinforced concrete beams*. Int. Conf. on *Recent Developments on the Fracture of Concrete and Rock* (20-22/9/1989), Cardiff, Wales, 1989, 672-681.
- [12] A. HILLERBORG - M. MODEER - P. E. PETERSSON, *Analysis of crack formation and crack growth in concrete by means of Fracture Mechanics and Finite Elements*. Cement and Concrete Research, 6, 1976, 773-782.

- [13] A. CARPINTERI, *Decrease of apparent tensile and bending strength with specimens size: two different explanations based on fracture mechanics*. Int. J. of Solid and Structures, vol. 25, 4, 1989, 407-429.
- [14] A. CARPINTERI, *Size effect in fracture toughness testing: a dimensional analysis approach*. In: G. C. SMITH - M. MIRABLE (eds.), Proc. Int. Conf. on *Analytical and Experim. Fracture Mechanics*. Sijthoff & Noordhoff, 1981, 785-797.
- [15] C. BOSCO - A. CARPINTERI - P. G. DEBERNARDI, *Minimum reinforcement in high-strength concrete*. J. of Structural Eng. (ASCE), vol. 116, 2, 1990, 427-437.
- [16] COMMISSION OF THE EUROPEAN COMMUNITIES, *Industrial Processes - Building and Civil Engineering*. Eurocode n. 2. Design of concrete structures. Part 1. General Rules and Rules for Buildings. October 1989.
- [17] AMERICAN CONCRETE INSTITUTE, *Building Code - Requirements for Reinforced Concrete (ACI 318-83)*, Detroit, Michigan, 1983.
- [18] K. SZALAI, *Principle of dimensioning of slightly-reinforced concrete structures*. Lectures presented at the 26th CEB Plenary Session, (20-23/9/1988), Dubrovnik 1988, 119-134.

Dipartimento di Ingegneria Strutturale
Politecnico di Torino
Corso Duca degli Abruzzi, 24 - 10129 TORINO